POSTPRINT

Late-Holocene ultra-distal cryptotephra discoveries in varved sediments of Lake Żabińskie, NE Poland

Małgorzata Kinder[a], Sabine Wulf[b], Oona Appelt[c], Mark Hardiman[b], Maurycy Żarczyński[a], Wojciech Tylmann[a]

[a] Faculty of Oceanography and Geography, University of Gdańsk, Bażyńskiego 4, 80-309 Gdańsk, Poland; malgorzata.kinder@ug.edu.pl

[b] School of the Environment, Geography and Geosciences, University of Portsmouth, Buckingham Building, Lion Terrace, Portsmouth, PO1 3HE, United Kingdom

[c] Helmholtz Centre Potsdam, GFZ German Research Centre for Geosciences, Section 3.6 Chemistry and Physics of Earth Materials, Telegrafenberg, D-14773 Potsdam, Germany

Abstract

Varved (annually laminated) lake sediments provide valuable archives for ultra-distal tephra preservation and at the same time allow the precise dating of volcanic eruptive events. We used a high-precision varve chronology from Lake Żabińskie in NE Poland and EPMA glass chemical data to identify cryptotephra from three large-scale, late Holocene eruptions from European and Northern American volcanoes: the White River Ash eastern lobe (WRAe) eruption from Mount Churchill, Alaska (AD 833-850); a tentative finding of the Glen Garry eruption of the Askja volcano, Iceland (1966-2210 cal a BP); and an yet undefined eruption from Furnas volcano, Azores. The varve age of AD 863-903 of the Alaskan WRAe cryptotephra in Lake Żabińskie is slightly younger than the proximal radiocarbon date and the annual layer estimate of the distal AD860B correlative in the Greenland NGRIP ice core but is within ^{14}C dating uncertainties of distal tephra findings in the Irish peat record. The varve ages of the Glen Garry and Furnas tephras in Lake Żabińskie provide a minimum age at 1991 cal a BP (41 BC). All three cryptotephra findings represent their easternmost occurrences from the volcanic source and hence considerably extend existing tephra dispersal maps.

Keywords:

cryptotephra; Askja; Mount Churchill; Azores; varved sediments; northeastern Poland

1. Introduction

Tephra (volcanic fall material) from explosive eruptions can be transported significant distances from the source volcano and therefore can provide a valuable tool for the dating and synchronisation of sedimentary records (Lowe, 2011). In recent palaeoclimatic investigations, for example, Lateglacial tephras have been used as isochrones to obtain first information about spatio-temporal relationships between climate variability and environmental responses in larger regional transects across northern and central Europe (e.g., Lane et al., 2013; Wulf et al., 2013; Rach et al., 2014). In fact, numerous tephra studies during the last three decades have shown that continental northwestern, northeastern and central Europe was regularly impacted by large-scale eruptions from Icelandic volcanoes and the Eifel Volcanic Field in western Germany since the Late Glacial (e.g., Mangerud et al., 1984; van den Bogaard and Schmincke, 2002; Davies et al., 2003; Wastegård, 2005; Haflidason et al., 2018), demonstrating the potential for extending palaeoclimate record comparisons also into the Holocene period. In Poland, the furthest easterly tephra dispersal was for long restricted to sites located on the western border (Fig. 1) and was limited by the identification of only macroscopic, visible ash layers, i.e. the 12.9 ka BP Eifel Laacher See Tephra (e.g., Juvigné et al., 1995). The methodological and analytical advances in cryptotephra identification (e.g., Turney, 1998; Blockley et al., 2008; Abbott and Davies, 2012; Davies, 2015) have recently allowed for the detection of both very small (<80 µm) and very low concentrations of tephra glass shards in Holocene sediment records further to the East, i.e. in sites in north-western and central Poland (e.g., Housley et al., 2013; Wulf et al., 2013, 2016; Watson et al., 2017a, 2017b) (Fig. 1). Specifically for the Late Holocene period these tephra findings include the AD1875 and the Glen Garry tephras (2088 ± 122 cal a BP; Barber et al., 2008; Gudmundsdóttir et al., 2016) from the Askja volcano in western Iceland, but also the WRAe tephra from Mount Churchill, Alaska (AD 833-850; Jensen et al., 2014), demonstrating the presence of tephra from even transcontinental volcanic sources in central-eastern Europe. Notably, the WRAe eruption has been recently associated by Jensen et al. (2014) with the distal AD860B tephra which has been identified in several northern European peat bogs (e.g., Pilcher et al., 1995, 1996; van den Bogaard and Schmincke, 2002; Lawson et al., 2012) and in the Greenland NGRIP ice record where it is dated at AD 853-855 (Coulter et al., 2012; Toohey and Sigl, 2017).

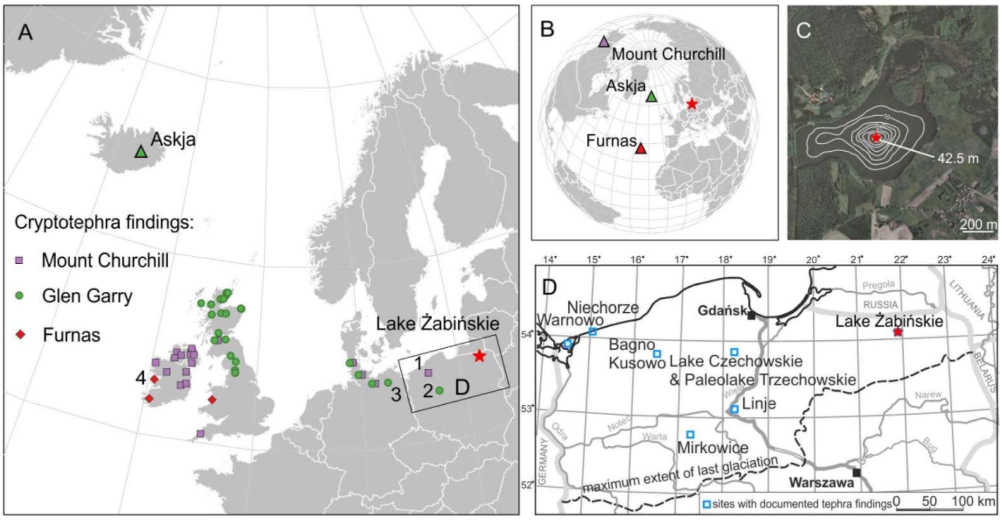

Figure 1. (A-B) Location of Mount Churchill, Askja and Furnas volcanoes and European tephra findings. Numbered sites are mentioned in the text: (1) Bagno Kusowo (Watson et al., 2017a), (2) Mirkowice (Housley et al., 2014), (3) Tiefer See (Dräger et al., 2017; Wulf et al., 2016), (4) An Loch Mór (Chambers et al., 2004); (C) surroundings and bathymetry of Lake Żabińskie. The red star indicates the coring site of core ZAB-12. (D) tephra findings in northern Poland: Warnowo, Niechorze (Juvigné et al., 1995), Lake Czechowskie, Trzechowskie Paleolake (Wulf et al., 2013, 2016), Linje (Watson et al., 2017a).

With the aim to extend the knowledge about the occurrence and dispersal of above mentioned Late Holocene tephras further east, varved sediments of Lake Żabińskie in northeastern Poland have been systematically inspected for their cryptotephra content. In this study, we present the glass chemical results of three cryptotephras found in the youngest sediments, covering the last ca. 2100 years.

2. Study site

Lake Żabińskie is a small (0.42 km^2) and deep lake (maximum depth of 44.4 m) located in the Masurian Lake District in northeastern Poland (54°07’54″N; 21°59’01″E) (Fig. 1). The landscape was formed during the Pomeranian phase of the Weichselian glaciation (ca. 16–15 ka BP; Szumański, 2000). The study site is well known for its excellent preservation of varved sediments, which have been extensively investigated for palaeoclimatic and environmental reconstructions (e.g., Amann et al., 2014; Bonk et al., 2016; Wacnik et al., 2016; Hernández-Almeida et al., 2017; Żarczyński et al., 2019).

Lake Żabińskie is positioned approximately 2300 km southeast of Iceland, ca. 3900 and 6200 km east of the Azores and Alaskan high-explosive volcanoes (Fig. 1), hence representing a site in an ultra-distal (>2000 km) location for receiving tephra fallout from any of those volcanic centres. A previous study on the uppermost organic-rich, annually laminated sediments of Lake Żabińskie has proven the presence of the historical Askja AD1875 cryptotephra from Iceland (Tylmann et al., 2016).

3. Material and methods

Composite sediment core ZAB-12 was retrieved from the deepest part of Lake Żabińskie (Fig. 1) in 2012 using a UWITEC piston corer (ø90 mm), which was operated from the floating platform. An age-depth model for the uppermost 5.95 m (last 2028 +34/-53 years) of core ZAB-12 based on varve counting and validated with radiocarbon dating was constructed by Żarczyński et al. (2018), which was extended in this study with 77 additional varves counted to 6.12 m depth covering the time period of the last ca. 2100 years. A targeted sediment sampling was carried out in order to search for tephras that have been previously reported in other sites in northern-central Europe and Poland (Fig. 1), namely the above-mentioned Alaskan WRAe/AD860B and Icelandic Glen Garry tephras. Because of the estimated uncertainty of the varve chronology of 4.3 % (Żarczyński et al., 2018) and the relatively low precision of the Glen Garry eruption age (2088 ± 122 cal a BP; Barber et al., 2008), the following two core sediment sections were chosen for targeted tephra sampling: core ZAB-12/5-2, 151 cm to 181 cm depth for the WRAe/AD860B tephra and core ZAB-12/4-3, 58 cm to 120 cm for the Glen Garry tephra. The selected sediment sections were sampled in contiguous 1 cm intervals with a volume of 1 cm^3 and chemically pre-treated with 30% H_2O_2 overnight in order to remove organic matter. Subsequently, a 7-10% HCl solution was added for a maximum of 1 hour to dissolve carbonates, and a 2M Na_2CO_3 solution was used for 6-7 hours in a 70-80°C water bath to dissolve biogenic silica (diatoms) instead of more aggressive NaOH (Rose et al., 1996; Davies et al., 2003; Clymans et al., 2015). The remaining material was wet-sieved, and the 20-100 µm grain size fraction was transposed to transparent plastic boxes for microscopic inspection of volcanic glass. In case of light organic matter remains or larger amount of minerogenic material, an additional step of liquid density separation (sodium polytungstate) at 1.95 and 2.55 g cm^{-3} was applied using the method after Blockley et al. (2005). Wet samples were inspected under a polarizing microscope (AXIO Imager A2, Zeiss) at 200× magnification. Counts of detected glass shards were expressed as shards per cubic cm of wet sediment. Identified glass shards were picked in a water medium with a 5 ml gas chromatography syringe and a 110 µm diameter micromanipulator needle (see method after Lane et al., 2014), then embedded in epoxy resin (Epofix™) in a single-hole aluminium stub and sectioned and polished prior to electron probe microanalyses (EPMA). The major-element composition of individual glass shards was obtained by a wavelength-dispersive spectrometry (WDS) JEOL-JXA8230 probe (15 kV voltage, 10 nA beam current and 1-4 µm beam diameter) at the GFZ Potsdam, Germany. Max Planck Institute (MPI) glass standards GOR-132, StHs6/80 and ATHO (Jochum et al., 2006) and the Lipari obsidian (Hunt and Hill, 1996; Kuehn et al., 2011) were measured prior to samples for analytical quality control (Table 1). EPMA data were normalised on an anhydrous and volatile-free basis to 100% and compared with tephra glass chemistries from specific eruptions from the literature (e.g., Chambers et al., 2004; Borgmark and Wastegård, 2008; Gjerløw et al., 2016) and the "Tephrabase" home page (www.tephrabase.org). Correlation of detected tephras used chemical bivariate plots and stratigraphic positions provided by the high-resolution varve chronology (Figs. 2,3). Tephras were labeled according to their core name, section and core depth, e.g. ZAB-12/5-2_160-162.

Table 1. EPMA major element composition of single glass shards from Lake Żabińskie assigned to known tephras and glass standards. The analysis in cursive (Glen Garry tephra) is probably an outlier.

Sample	SiO_2	TiO_2	Al_2O_3	FeO^t	MnO	MgO	CaO	Na_2O	K_2O	P_2O_5	Cl	Total	Beam size [μm]
WRAe/AD8 60B													
ZAB-12/5-2_ 153-154	69.83	0.24	13.17	1.50	0.06	0.42	1.79	2.83	2.94	0.05	0.27	93.09	3
	72.84	0.22	14.31	1.60	0.06	0.45	1.77	3.12	2.02	0.05	0.33	96.77	3
ZAB-12/5-2_ 160-161	66.96	0.22	14.11	1.57	0.03	0.51	1.55	3.24	2.73	0.07	0.33	91.32	2
	73.07	0.22	14.40	1.53	0.03	0.46	1.79	3.32	3.08	0.04	0.28	98.22	4
	72.43	0.27	14.46	1.68	0.06	0.41	1.70	3.15	3.17	0.09	0.31	97.72	4
	69.50	0.20	13.30	1.48	0.03	0.45	1.61	2.40	2.34	0.06	0.27	91.63	1
	74.38	0.22	15.04	1.52	0.02	0.36	1.71	1.90	2.56	0.07	0.31	98.09	1
	73.47	0.13	13.05	1.04	0.06	0.19	1.17	1.55	2.60	0.02	0.33	93.59	1
	71.37	0.24	13.69	1.55	0.05	0.38	1.75	2.57	2.56	0.06	0.34	94.57	1
Glen Garry													
ZAB-12/4-3_ 92-93	62.32	1.42	13.41	7.40	0.08	2.28	5.34	3.82	1.25	0.23	0.02	97.58	3
	71.92	0.61	12.43	4.20	0.09	0.48	2.18	2.57	1.46	0.14	0.02	96.09	3
	65.95	*0.50*	*14.53*	*6.05*	*0.18*	*0.64*	*2.91*	*2.75*	*1.70*	*0.13*	*0.03*	*95.38*	*3*
ZAB-12/4-3_ 93-94	74.55	0.52	12.50	3.99	0.08	0.50	2.09	2.88	1.56	0.08	0.02	98.78	3
Furnas													
ZAB-12/4-3_ 93-94	64.50	0.41	17.61	3.39	0.21	0.29	0.68	6.66	5.52	0.00	0.37	99.65	3
	63.29	0.42	17.42	3.72	0.35	0.30	0.70	5.33	5.31	0.05	0.34	97.23	3
	62.48	0.41	16.88	3.70	0.30	0.34	0.63	4.97	4.22	0.05	0.35	94.33	3
Glass Standards													
Lipari	74.54	0.06	12.92	1.53	0.04	0.06	0.69	3.71	4.96	0.00	0.32	98.82	10
	73.93	0.09	12.83	1.58	0.13	0.05	0.70	3.63	5.01	0.02	0.35	98.32	5
GOR-132	45.40	0.29	10.31	10.35	0.16	22.55	8.10	0.74	0.03	0.01	0.00	97.93	10
	46.05	0.31	10.77	10.44	0.14	22.32	8.21	0.74	0.00	0.01	0.01	99.00	5
StHs6/80	63.85	0.67	17.82	4.34	0.10	2.08	5.21	4.24	1.26	0.17	0.01	99.74	10
	63.84	0.71	17.67	4.19	0.05	2.14	5.08	4.18	1.21	0.19	0.02	99.29	5
ATHO	75.43	0.27	11.94	3.26	0.11	0.06	1.54	3.47	2.79	0.05	0.02	98.93	10
	75.77	0.25	11.89	3.34	0.13	0.09	1.69	3.54	2.80	0.05	0.03	99.58	5

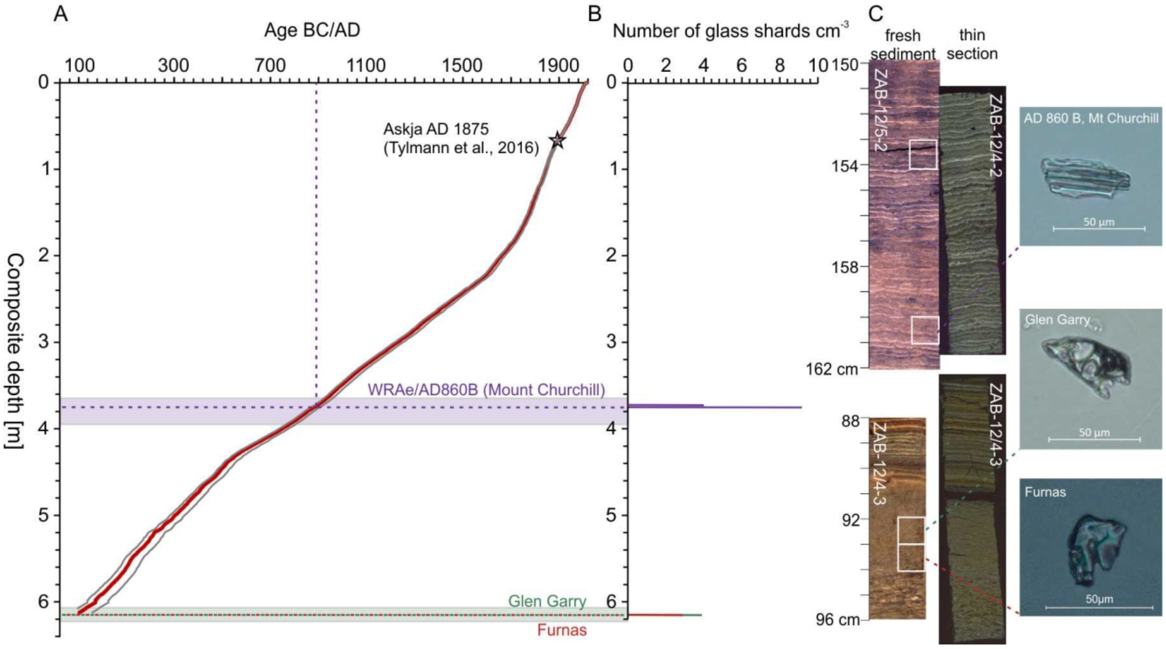

Figure 2. (A) Age-depth model based on varve chronology and (B) the number of volcanic glass shards with shaded bars representing sampled sections, (C) images of the sediment cores (ZAB-12/5-2 and ZAB-12/4-3) and thin sections (ZAB-12/4-2 and ZAB-12/4-3) with positions of new tephra findings and microscope images showing the examples from each cryptotephra (under polarized light).

4. Results

Three cryptotephra horizons with very low glass shard concentrations (n: 2-9) were detected and chemically analysed in the investigated core sections ZAB-12/5-2 and ZAB-12/4-3.

4.1 Cryptotephra layers ZAB-12/5-2_160-161 and ZAB-12/5-2_153-154 (WRAe/AD860B, Mount Churchill)

A total of nine and four glass shards cm^{-3} have been detected in a continuously varved sediment section at 375.5 cm and 369.2 cm composite depth, namely in samples ZAB 12/5-2_160-161 and ZAB 12/5-2_153-154 which are dated by varve counting at AD 877 +14/-26 and AD 912 +14/-26, respectively (Fig. 2). Normalized EPMA major element data of a total of ten analysed glass shards (eight from ZAB 12/5-2_160-161 and two from ZAB 12/5-2_153-154) showed that both tephra layers share the same high-silica rhyolitic composition which is characterized by relatively large concentration ranges of 73.3-78.5 wt% SiO_2, 19.9-15.5 wt% Al_2O_3, 1.1-1.7 wt% FeO, 1.2-1.9 wt% CaO, and alkali ratios (K_2O/Na_2O) of 0.6-1.7. This chemistry matches the glass composition of the Alaskan WRAe/AD860B tephra except for lower Na_2O and slightly elevated SiO_2 concentrations (Fig. 3, Table 1). The latter reflects alkali (sodium) migration during EPMA measurements (Nielsen and Sigurdsson, 1981; Hayward, 2012) that was likely caused by the small/thin nature of glass shards and the use of respective small electron beam size diameters (1-4 µm).

Because of the undisturbed (varved) character of sediments and the higher glass shards concentration in the lower ZAB 12/5-2_160-161 cryptotephra, the horizon at 375.5 cm composite depth has been defined as the primary fallout layer of the WRAe/AD860B eruption, while the upper tephra 12/5-2_153-154 is interpreted as redistributed material from shallower parts of the lake basin due to sediment focusing.

The occurrence of WRAe/AD860B glass shards in Lake Żabińskie over 6000 km from its volcanic source in Alaska clearly indicates a large-magnitude event and/or tephra dispersal by strong westerly winds. This White River Ash eastern lobe (WRAe) eruption was in fact one of the largest Plinian eruptions in the Holocene (VEI=6) with an ash cloud reaching ~45 km in height (Lerbekmo, 2008). The transatlantic distribution of the WRAe has been confirmed by the presence of the WRAe/AD860B tephra in eastern Canada (e.g., Jensen et al., 2014), in the Greenland NGRIP ice core (Coulter et al., 2012), in western Europe - mainly in the British Isles (e.g., Pilcher et al., 1995; Hall and Pilcher, 2002; Plunkett et al., 2004), in northern Germany (van den Bogaard and Schmincke, 2002) and in Bagno Kusowo bog in western Poland (Watson et al., 2017a) (Fig. 1). There are single sites of uncertain findings in Norway as well (Pilcher et al., 2005; Vorren et al., 2007). The new occurrence of the WRAe/AD860B tephra in Lake Żabińskie extends its dispersal fan another 300 km further to the east. The WRAe/AD860B tephra forms therewith a rare and valuable transatlantic isochron that can be used for comparing palaeoclimate records covering the onset of the Medieval Climatic Anomaly (e.g., Jensen et al., 2014).

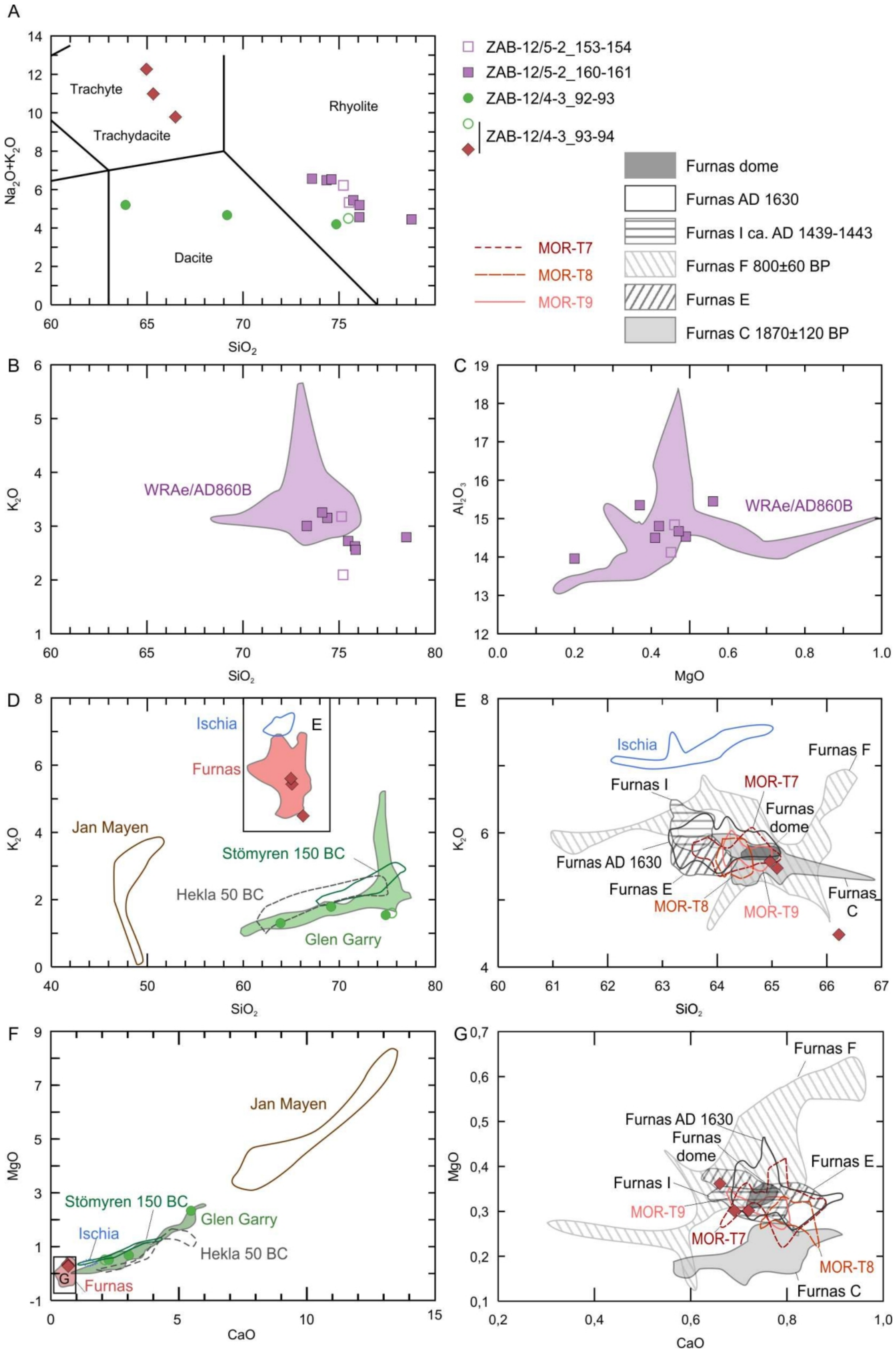

Figure 3. Bivariate plots of selected major elemental compositions (normalized data) of cryptotephra glass shards from Lake Żabińskie. (A) Total alkali-silica (TAS) diagram after Le Bas et al. (1986). (B, C) SiO_2 versus K_2O and MgO versus Al_2O_3 for tephras ZAB-12/5-2_153-154 and ZAB-12/5-2_160-161 in comparison with published data of the Alaskan WRAe/AD860B tephras. Reference data from

Tephrabase; Plunkett and Pilcher, 2018. (D-G) SiO_2 versus K_2O and CaO versus MgO in comparison with published data of tephras from Stömyren ca 150 BC (Wastegård, 2005), Furnas (Chambers et al., 2004; Andresson et al., 2016; Johansson et al., 2017; Wastegård et al., 2020), Glen Garry (Housley et al., 2014; Tephrabase), Hekla 50 BC (Borgmark and Wastegård, 2008; Watson et al., 2016), Ischia (de Alteriis et al., 2010), and Jan Mayen (Gjerløw et al., 2016).

4.2 Cryptotephra layers ZAB-12/4-3_ 93-94 and ZAB-12/4-3_ 92-93 (Glen Garry?, Askja)

Three out of six colorless and vesicular shards in sample ZAB-12/4-3_92-93 (613.5 cm composite depth) and one shard in sample ZAB 12/4-3_93-94 (614.5 cm composite depth) show a similar rhyodacitic composition with large concentration ranges in SiO_2 (63.9-75.5 wt%), FeO (4.0-.6 wt%) and CaO (2.3-5.5 wt%) (Fig. 3A, D, F, Table 1). This chemistry is typical for Icelandic tephras, and in particular matches the composition of the distal Glen Garry tephra (2088 ± 122 cal a BP; Barber et al., 2008). The source volcano of the Glen Garry tephra was uncertain for a long time; Askja volcano has been repeatedly proposed due to some similarities to the proximal Stömyren 150 BC tephra (e.g., Wastegård, 2005; Plunkett and Pilcher, 2018) but never confirmed until recent findings in sites in central Iceland which have associated the Glen Garry tephra with the A~2000 eruption of the Askja volcano (Gudmundsdóttir et al., 2016).

Because of the occurrence of Glen Garry glass shards in both samples (92-94 cm core depth), a mean core depth of 93 cm (614 cm composite depth) has been chosen for defining the position of the tephra isochron in the Lake Żabińskie sequence. The lithology in this section is characterized by a transition from a 65-cm-thick mass-movement deposit that consists of folded varved sediments and an 8-cm thick turbidite at the top of the slump to varved, organic-rich sediments. The Glen Garry tephra occurs within the uppermost 2-3 cm of the turbidite, which is varve dated at 94 BC (+34/-53 years) or 2078-1991 cal a BP. The mass-movement deposit may have been most likely caused by a gravity underflow related to slope overloading.

Dispersal of the Glen Garry tephra was for long limited to Scotland (e.g., Dugmore et al., 1995; Langdon and Barber, 2001, 2004; Barber et al., 2008; Lawson et al., 2012), northern England (Pilcher and Hall, 1996), and northern Germany (e.g., van den Bogaard and Schmincke, 2002; Wulf et al., 2016), and has only recently been extended to the site of Mirkowice in western Poland (Housley et al., 2014) (Fig. 1A, D). With the finding in Lake Żabińskie it has been identified in a new site in northeastern Poland enabling the extension of the Glen Garry ash tephra fall axis over 300 km eastwards. Further tephra detection in other northern and central European records would help to synchronize palaeo-proxy data focusing on the last three millennia.

4.3 Cryptotephra ZAB-12/4-3_ 93-94 (Furnas, Azores)

Sample ZAB 12/4-3_93-94 in 614.5 cm composite depth contains an additional glass population (n=3) with a distinct trachytic composition that is characterized by relatively narrow concentration ranges in SiO_2 (65.0-66.2 wt%), low MgO (~0.3 wt%) and CaO (~0.7 wt%) values, relatively high FeO concentrations (~3.4-3.7 wt%), and total alkalis (Na_2O+K_2O) of ~11 wt% (Fig. 3A, D-G). Comparisons with trachytic glass chemistries of Late Holocene tephras from potential volcanic sources exclude an origin from Jan Mayen and Ischia (southern Italy) due to considerably lower SiO_2 concentrations (Jan Mayen) and higher CaO and Al_2O_3 values (Ischia) (Fig. 3D-G). However, a very good match of the trachytic ZAB 12/4-3_93-94 glass component is given with proximal tephras from Furnas volcano, Azores (e.g., Wastegård et al., 2020) and with three Late Holocene distal tephras, MOR-T7, -T8 and -T9, from the An Loch Mór lake record in western Ireland (Chambers et al., 2004) (Fig. 3D-G). MOR-T7 to -T9 tephras, dated between AD 35 (1915 cal a BP; MOR-T9) and AD 280 (1670 cal a BP; MOR-T7), have been originally associated with Jan Mayen (Chambers et al., 2014) but more recently correlated with Furnas activities (Johansson et al., 2017; Plunkett and Pilcher, 2018). Furnas is one out of three volcanic centers on São Miguel Island, Azores, which had at least 5 explosive eruptions and dispersal of tephra during the past 5600 years (e.g., Guest et al., 1999; Jones et al., 1999; Guest et al., 2015). New proximal glass data of these tephras indicate similar trachytic major element compositions that complicate the correlation of distal tephra findings with specific Furnas volcanic events (Johansson et al., 2017; Wastegård et al., 2020). During the deposition of the Lake Żabińskie tephra at 2078-1991 cal a BP (94 BC +34/-53), two potential Furnas eruptions occurred: Furnas B at 2470-2150 cal a BP (520-200 BC; Cole et al., 1999; Wastegård et al., 2020), and Furnas C at 2115-1542 cal a BP (165 BC – AD 412; Guest et al., 1999), with Furnas C being proposed the larger (VEI=5) eruption with a strong tephra dispersal towards the North (Guest et al., 2015). Johansson et al. (2017) tentatively correlated Furnas C with the distal Irish tephras MOR-T7, -T8 and -T9, while the older Furnas B eruption has been associated on a chronostratigraphical basis with the distal tephra DCSH-2 in Derrycunihy, Ireland, which is radiocarbon interpolated at 465-365 BC (Reilly and Mitchell, 2015).

The glass chemical results clearly assign Furnas as the source volcano for the trachytic ZAB 12/4-3_93-94 tephra, but the exact eruptive event is difficult to determine due to the lack of Furnas B glass chemical data. At this point, only a tentative correlation can be suggested with one of the distal MOR-T7, -T8 or- T9 tephras (AD 35 to AD 280; or 1915 to 1670 cal a BP), which approximate both the age and chemistry of the trachytic ZAB 12/4-3_93-94 tephra. This is despite slightly lower sodium and potassium concentrations of one shard in ZAB 12/4-3_93-94 in comparison to the other two data points, which again likely resulted from analytical difficulties to obtain reliable data from an extremely small glass shard in this ultra-distal tephra.

The occurrence of several Furnas tephra layers in peat and lake sediments in Ireland (Chambers et al., 2004, Reilly and Mitchell, 2015) and the new findings in Lake Żabińskie (this study) indicate frequent eruptions from Azorean volcanoes and prevailing favorable wind conditions towards the North and Northeast linked to the North Atlantic Oscillation (Hurrell et al., 2003).

5. Dating of tephra layers

5.1 WRAe/AD860B tephra

The distal equivalent of the Alaskan WRAe tephra, the AD860B tephra, has been first detected in association with the Icelandic AD860A tephra in Irish peat sediments (Pilcher et al., 1995) and was only recently correlated with the White River Ash eastern lobe (WRAe) of Mount Churchill volcano (Jensen et al., 2014). Even though "AD860B" is an estimated age, it has been widely replicated (Swindles et al., 2013; Davies, 2015; Watson et al., 2016, 2017a). Therefore, a combined name WRAe/AD860B used by Jensen et al. (2014) may be considered for future studies. Several age estimates are currently available for the WRAe/AD860B tephra (Fig. 4). Pilcher et al. (1995) originally constrained an age at AD 860 ± 20 (AD 776-887, 2σ) on the basis of multi-sample radiocarbon wiggle matching of ombrogenous peat containing the tephra in the Irish bogs. Proximal WRAe deposits have been recently dated at AD 833-850 by wiggle-matching multiple radiocarbon dates on tree rings from a spruce killed by the eruption (Jensen et al., 2014). Patterson et al. (2017) presented an offset of the WRAe tephra in radiocarbon age models from the Canadian Subarctic due to the freshwater reservoir effect. In the NGRIP Greenland ice core, the timing of the WRAe/AD860B tephra has been pinpointed by the GICC05 chronology to AD 847 ± 1 (AD 846-848; Coulter et al., 2012). However, Baillie (2008) and Sigl et al. (2015) proposed an offset of the GICC05 by 6 years within this time interval and consequently a new, more precise age of AD 853-855 has been provided (Toohey and Sigl, 2017). The varve age of the WRAe/AD860B tephra in Lake Żabińskie at AD 877 +14/-26 (AD 863-903) is consistent and within a 2σ dating uncertainty with the initial date obtained by Pilcher et al. (1995), but it is slightly younger (≥8-13 years) than the corrected Greenland ice core date and the radiocarbon date from the proximal site (Jensen et al., 2014) (Fig. 4). This may have been caused by: 1) underestimation of the varve counts in Lake Żabińskie by missing varves or sedimentary gaps; 2) overestimation of annual layers in the NGRIP ice core record; or 3) radiocarbon dating uncertainties through volcanogenic CO_2 contamination of the proximal WRAe/AD860B tephra.

An underestimation of the tephra age by the Lake Żabińskie varve chronology can be likely excluded, because varve count uncertainties of the WRAe/AD860B tephra are already included, and the continuously varved sediment sequence does not show any evidence of depositional gaps. This can be corroborated by an additional radiocarbon date obtained from a pine bark 1 cm above the WRAe/AD860B cryptotephra in Lake Żabińskie, yielding an age at AD 888-990 (95.4%; 1070±30 ^{14}C a

BP) which is in agreement with the varve age and its uncertainty at the same depth at AD 874-910 (Żarczyński et al., 2018).

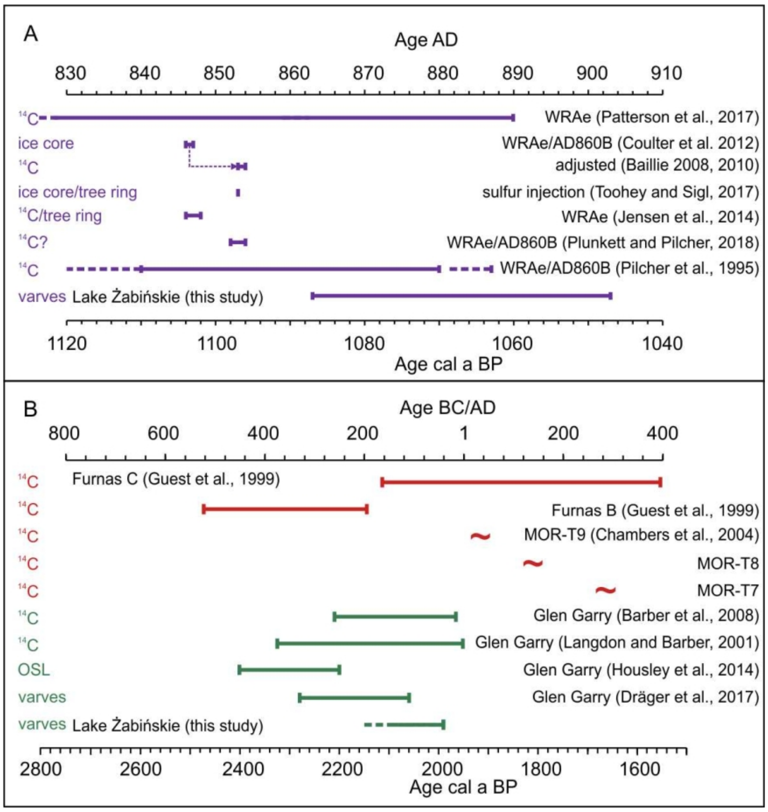

Figure 4. Schematic representation of age estimates for the WRAe/AD860B (A), Furnas and Glen Garry (B) tephras from published records (Pilcher et al., 1995; Guest et al., 1999; Langdon and Barber, 2001; Chambers et al., 2004; Baillie, 2008; Barber et al., 2008; Baillie, 2010; Coulter et al., 2012; Housley et al., 2014; Jensen et al., 2014; Dräger et al., 2017; Patterson et al., 2017; Toohey and Sigl, 2017; Plunkett and Pilcher, 2018), and new data from this study.

5.2 Glen Garry tephra

The Glen Garry tephra was first identified in peat and lake sediments in Scotland (e.g., Dugmore and Newton, 1995; Langdon and Barber, 2001, 2004), followed by other findings in northern England (Pilcher and Hall, 1996), northern Germany (van den Bogaard and Schmincke, 2002; Wulf et al., 2016), and in a single archeological site in Mirkowice in western Poland (Housley et al., 2014) (Fig. 1). Despite the relatively large number of findings, dating of the Glen Garry tephra is still problematic. First radiocarbon dates gave three age ranges of the Glen Garry tephra: 1827-2111, 1940-2309 and 2006-2350 cal a BP (Dugmore et al., 1995; Dugmore and Newton, 1995; Pilcher and Hall, 1996). A mean age of the Glen Garry tephra has been estimated to 2088 ± 122 cal a BP (260-16 BC; Barber et al., 2008), with a 2σ range of 2210-1966 cal a BP. Housley et al. (2014) provided an OSL age of the Glen Garry tephra in Mirkowice at 2300 ± 100 years. The horizon containing the Glen Garry cryptotephra in Lake Tiefer See (NE Germany) was dated to 2170 ± 110 cal a BP on the basis on varve counting and interpolation of accumulation rates in poorly laminated sediment sections (Wulf et al., 2016; Dräger et al., 2017) (Fig. 4). Continuous varve counting provided a date of the Glen Garry tephra in Lake Żabińskie at 2078-1991 cal a BP (94 BC +34/-53). However, due to the fact that this cryptotephra is located at the top of a slump which had interrupted the varved structure, tephra shard re-deposition cannot be excluded. Hence, a minimum age of the Glen Garry tephra can be proposed at 1991 cal a BP (41 BC), which narrows down the upper limit of tephra radiocarbon dates presented in previous studies by Langdon and Barber (2001) and Barber et al. (2008). The current dating uncertainty still shows a strong need for refining the age of the Glen Garry tephra.

5.3 Furnas tephra

The Furnas tephra in Lake Żabińskie was likely erupted contemporary with the Glen Garry tephra due to its finding in the same sediment sample; however, this interpretation has to be treated with caution due to slumping and possible mixing of material of different age. Unfortunately, there is no other site with both tephras identified and undisturbed record allowing to resolve the stratigraphic order of the Glen Garry and Furnas tephras. The closest chemical and chronostratigraphical correlatives of the Furnas tephra in Lake Żabińskie are the distal MOR-T7, -T8 or -T9 tephras which are dated between 1915 and 1670 cal a BP (AD 35 to AD 280; Chambers et al., 2004) and associated with the Furnas C eruption (Johansson et al., 2017). The MOR-T7 to MOR-T9 ages were constrained by geochemical indicators of smelting in the Roman Empire and palynological evidences of the Late Iron Age Lull (AD 1-200) and consider uncertainties of up to 50 years (Chambers et al., 2004). The Furnas tephra in Lake Żabińskie has a minimum age of 1991 cal a BP (41 BC) and therefore may tentatively relate to the oldest MOR-T9 tephra (Fig. 4B). However, due to its position within a mass-movement deposit in Lake Żabińskie, a more precise age of this eruption cannot be constrained. Hence, other records with precise chronologies are needed to verify both the correlation and timing of both tephras.

6. Conclusions

Systematic searches and major element glass analyses have identified three cryptotephras of different provenance in late Holocene, varved sediments from Lake Żabińskie in northeastern Poland: (1) the ultra-distal tephra from the Alaskan WRAe/AD860B (Mount Churchill) eruption, (2) tentatively the Icelandic Glen Garry tephra, and (3) an Azorean tephra from Furnas volcano that likely erupted contemporary to the Glen Garry tephra and that may relate to any of the distal MOR-T7, -T8, -T9 tephras in the Irish lacustrine record. Varve counting of the Lake Żabińskie sediments date the

WRAe/AD860B tephra to AD 863-903 and suggests a minimum age for the Glen Garry and Furnas tephras of 1991 cal a BP (41 BC).

The new cryptotephra findings in the late Holocene sediments of Lake Żabińskie extend the dispersal maps of each tephra further east, hence providing information for a better understanding of past air mass trajectories. Furthermore, the detection of the late Holocene Furnas tephra in eastern Poland shows a new potential for identifying Azorean tephras also in other records from western and central Europe.

Acknowledgements

We would like to thank Stefan Wastegård and an anonymous reviewer for their mindful and constructive comments and suggestions for improving earlier versions of this manuscript. This work was supported by the Polish National Science Centre (grant number 2015/19/D/ST10/02854) and the University of Gdańsk (grant number 538-G110-B101-18).

References

Abbott, P.M., Davies, S.M., 2012. Volcanism and the Greenland ice-cores: the tephra record. Earth-Sci Rev 115, 173–191. https://doi.org/10.1016/J.EARSCIREV.2012.09.001.

Amann, B., Lobsiger, S., Fischer, D., Tylmann, W., Bonk, A., Filipiak, J., Grosjean, M., 2014. Spring temperature variability and eutrophication history inferred from sedimentary pigments in the varved sediments of Lake Żabińskie, north-eastern Poland, AD 1907–2008. Global Planet Change 123, 86–96. https://doi.org/10.1016/J.GLOPLACHA.2014.10.008.

Andersson, T., Hermelin, O., Skelton, A., Jakobsson, M., 2016. Bottom characterization of Lagoa das Furnas on São Miguel, Azores archipelago. J Volcanol Geotherm Res 321, 196–207.

Baillie, M.G., 2008. Proposed re-dating of the European ice core chronology by seven years prior to the 7th century AD. Geophys Res Lett 35, L15813. https://doi.org/10.1029/2008GL034755.

Baillie, M.G., 2010. Volcanoes, ice-cores and tree-rings: one story or two? Antiquity 84, 202–215. https://doi.org/10.1017/S0003598X00099877.

Barber, K., Langdon, P., Blundell, A., 2008. Dating the Glen Garry tephra: A widespread late-Holocene marker horizon in the peatlands of northern Britain. Holocene 18, 31–43. https://doi.org/10.1177/0959683607085594.

Blockley, S.P.E., Pyne-O'Donnell, S.D.F., Lowe, J.J., Matthews, I.P., Stone, A., Pollard, A.M., Turney, C.S.M., Molyneux, E.G., 2005. A new and less destructive laboratory procedure for the physical separation of distal glass tephra shards from sediments. Quat Sci Rev 24, 1952–1960. https://doi.org/10.1016/j.quascirev.2004.12.008.

Blockley, S.P.E., Bronk Ramsey, C., Pyle, D.M., 2008. Improved age modelling and high-precision age estimates of late Quaternary tephras, for accurate palaeoclimate reconstruction. J Volcanol Geotherm Res 177, 251–262. https://doi.org/10.1016/j.jvolgeores.2007.10.015.

Bonk, A., Kinder, M., Enters, D., Grosjean, M., Meyer-Jacob, C., Tylmann, W., 2016. Sedimentological and geochemical responses of Lake Żabińskie (north-eastern Poland) to erosion changes during the last millennium. J Paleolimnol 56, 239–252. https://doi.org/10.1007/s10933-016-9910-6.

Borgmark, A., Wastegård S., 2008. Regional and local patterns of peat humification in three raised peat bogs in Värmland, south-central Sweden, GFF 130, 161–176. DOI: 10.1080/11035890809453231.

Chambers, F.M., Daniell, J.R.G., Hunt, J.B., Molloy, K., O'Connell, M., 2004. Tephrostratigraphy of An Loch Mór, Inis Oírr, western Ireland: Implications for Holocene tephrochronology in the northeastern Atlantic region. Holocene 14, 703–720. https://doi.org/10.1191/0959683604hl749rp.

Clymans, W., Barão, L., Van der Putten, N., Wastegård, S., Gísladóttir, G., Bjorck, S., Moine, B., Struyf, E., Conley, D. J. 2015. The contribution of tephra constituents during biogenic silica determination: implications for soil and palaeoecological studies. Biogeosciences 12, 3789–3804. https://doi.org/10.5194/bg-12-3789-2015.

Coulter, S.E., Pilcher, J.R., Plunkett, G., Baillie, M., Hall, V.A., Steffensen, J.P., Vinther, B.M., Clausen, H.B., Johnsen, S.J., 2012. Holocene tephras highlight complexity of volcanic signals in Greenland ice cores. J Geophys Res Atmos 117, D21303. https://doi.org/10.1029/2012JD017698.

Davies, S.M., 2015. Cryptotephras: The revolution in correlation and precision dating. J Quat Sci 30, 114–130. https://doi.org/10.1002/jqs.2766.

Davies, S.M., Wastegård, S., Wohlfarth, B., 2003. Extending the limits of the Borrobol Tephra to Scandinavia and detection of new early Holocene tephras. Quat Res 59, 345–352. https://doi.org/10.1016/S0033-5894(03)00035-8.

De Alteriis, G., Insinga, D., Morabito, S., Morra, V., Chiocci, F.L., Terrasi, F., Lubritto, C., Di Benedetto, C., Pazzanese, M., 2010. Age of submarine debris avalanches and tephrostratigraphy offshore Ischia Island, Tyrrhenian Sea, Italy. Mar Geol 278, 1–18. https://doi.org/10.1016/j.margeo.2010.08.004.

Dräger, N., Theuerkauf, M., Szeroczyńska, K., Wulf, S., Tjallingii, R., Plessen, B., Kienel, U., Brauer, A., 2017. Varve microfacies and varve preservation record of climate change and human impact for the last 6000 years at Lake Tiefer See (NE Germany). Holocene 27, 450–464. https://doi.org/10.1177/0959683616660173.

Dugmore, A.J., Newton, A.J., 1995. Seven tephra isochrones in Scotland. Holocene 5, 257–266. https://doi.org/10.1177%2F095968369500500301.

Dugmore, A.J., Shore, J.S., Cook, G.T., Newton, A.J., Edwards, K.J., Larsen, G., 1995. The radiocarbon dating of tephra layers in Britain and Iceland. 15th Int C Conf 37, 379–388. https://doi.org/10.1017/S003382220003085X.

Gjerløw, E., Haflidason, H., Pedersen, R.B., 2016. Holocene explosive volcanism of the Jan Mayen (island) volcanic province, North-Atlantic. J Volcanol Geotherm Res 321, 31–43. https://doi.org/10.1016/J.JVOLGEORES.2016.04.025.

Gudmundsdóttir, E.R., Larsen, G., Björck, S., Ingólfsson, Ó., Striberger, J., 2016. A new high-resolution Holocene tephra stratigraphy in eastern Iceland: Improving the Icelandic and North Atlantic tephrochronology. Quat Sci Rev 150, 2341–249. https://doi.org/10.1016/j.quascirev.2016.08.011.

Guest, J., Gaspar, J., Cole, P., Queiroz, G., Duncan, A., Wallenstein, N., Ferreira, T., Pacheco, J.-M., 1999. Volcanic geology of Furnas Volcano, São Miguel, Azores. J Volcanol Geotherm Res 92, 1–29. https://doi.org/10.1016/S0377-0273(99)00064-5.

Guest, J. E., Pacheco, J. M., Cole, P. D., Duncan, A. M., Wallenstein, N., Queiroz, G., Gaspar, J.L., Ferreira, T., 2015. Chapter 9 The volcanic history of Furnas Volcano, São Miguel, Azores. Geol Soc London, Mem 44, 125–134. https://doi.org/10.1144/m44.9.

Haflidason, H., Regnéll, C., Pyne-O'Donnell, S., Svendsen, J. I., 2019. Extending the known distribution of the Vedde Ash into Siberia: occurrence in lake sediments from the Timan Ridge and the Ural Mountains, northern Russia. Boreas 48, 444–451. https://doi.org/10.1111/bor.12354.

Hall, V.A., Pilcher, J.R., 2002. Late-Quaternary Icelandic tephras in Ireland and Great Britain: detection, characterization and usefulness. Holocene 12, 223–230. https://doi.org/10.1191%2F0959683602hl538rr.

Hayward, C., 2012. High spatial resolution electron probe microanalysis of tephras and melt inclusions without beam-induced chemical modification. Holocene 22, 119–125. https://doi.org/10.1177%2F0959683611409777.

Hernández-Almeida, I., Grosjean, M., Gómez-Navarro, J.J., Larocque-Tobler, I., Bonk, A., Enters, D., Ustrzycka, A., Piotrowska, N., Przybylak, R., Wacnik, A., Witak, M., Tylmann, W., 2017. Resilience, rapid transitions and regime shifts: Fingerprinting the responses of Lake Żabińskie (NE Poland) to climate variability and human disturbance since AD 1000. Holocene 27, 258–270. https://doi.org/10.1177/0959683616658529.

Housley, R.A., MacLeod, A., Armitage, S.J., Kabaciński, J., Gamble, C.S., 2014. The potential of cryptotephra and OSL dating for refining the chronology of open-air archaeological windblown sand sites: A case study from Mirkowice 33, northwest Poland. Quat Geochronol 20, 99–108. https://doi.org/10.1016/j.quageo.2013.11.003.

Housley, R.A., MacLeod, A., Nalepka, D., Jurochnik, A., Masojć, M., Davies, L., Lincoln, P.C., Bronk Ramsey, C., Gamble, C.S., Lowe, J.J., 2013. Tephrostratigraphy of a Lateglacial lake sediment sequence at Węgliny, southwest Poland. Quat Sci Rev 77, 4–18.

https://doi.org/10.1016/j.quascirev.2013.07.014.

Hunt, J.B., Hill, P.G., 1996. An inter-laboratory comparison of the electron probe microanalysis of glass geochemistry. Quat Int 34–36, 229–241. https://doi.org/10.1016/1040-6182(95)00088-7.

Hurrell, J.W., Kushnir, Y., Ottersen, G., Visbeck, M., 2003. An Overview of the North Atlantic Oscillation, in: The North Atlantic Oscillation: Climatic Significance and Environmental Impact. American Geophysical Union, pp. 1–36.

Jensen, B.J.L., Pyne-O'Donnell, S., Plunkett, G., Froese, D.G., Hughes, P.D.M., Sigl, M., McConnell, J.R., Amesbury, M.J., Blackwell, P.G., van den Bogaard, C., Buck, C.E., Charman, D.J., Clague, J.J., Hall, V.A., Koch, J., Mackay, H., Mallon, G., McColl, L., Pilcher, J.R., 2014. Transatlantic distribution of the Alaskan White River Ash. Geology 42, 875–878. https://doi.org/10.1130/G35945.1.

Jochum, K.P., Stoll, B., Herwig, K., Willbold, M., Hofmann, A.W., Amini, M., Aarburg, S., Abouchami, W., Hellebrand, E., Mocek, B., Raczek, I., Stracke, A., Alard, O., Bouman, C., Becker, S., Dücking, M., Brätz, H., Klemd, R., de Bruin, D., Canil, D., Cornell, D., de Hoog, C.-J., Dalpé, C., Danyushevsky, L., Eisenhauer, A., Gao, Y., Snow, J.E., Groschopf, N., Günther, D., Latkoczy, C., Guillong, M., Hauri, E.H., Höfer, H.E., Lahaye, Y., Horz, K., Jacob, D.E., Kasemann, S.A., Kent, A.J.R., Ludwig, T., Zack, T., Mason, P.R.D., Meixner, A., Rosner, M., Misawa, K., Nash, B.P., Pfänder, J., Premo, W.R., Sun, W.D., Tiepolo, M., Vannucci, R., Vennemann, T., Wayne, D., Woodhead, J.D., 2006. MPI-DING reference glasses for in situ microanalysis: new reference values for element concentrations and isotope ratios. G-cubed 7. Q02008.

Johansson, H., Lind, E.M., Wastegård, S., 2017. Compositions of glass in proximal tephras from eruptions in the Azores archipelago and their links with distal sites in Ireland. Quat Geochronol 40, 120–128. https://doi.org/10.1016/j.quageo.2016.07.006.

Jones, G., Chester, D., Shooshtarian, F., 1999. Statistical analysis of the frequency of eruptions at Furnas Volcano, São Miguel, Azores. J Volcanol Geotherm Res 92, 31–38. https://doi.org/10.1016/S0377-0273(99)00065-7.

Juvigné, É., Kozarski, S., Nowaczyk, B., 1995. The occurrence of Laacher See Tephra in Pomerania, NW Poland. Boreas. https://doi.org/10.1111/j.1502-3885.1995.tb00775.x.

Kuehn, S. C., Froese, D. G., Shane, P. A. R., INTAV Intercomparison Participants, 2011. The INTAV intercomparison of electron-beam microanalysis of glass by tephrochronology laboratories: results and recommendations. Quat Int 246, 19–47. https://doi.org/10.1016/j.quaint.2011.08.022.

Lane, C. S., Brauer, A., Blockley, S. P., Dulski, P., 2013. Volcanic ash reveals time-transgressive abrupt climate change during the Younger Dryas. Geology 41, 1251–1254. https://doi.org/10.1130/G34867.1.

Lane, C. S., Cullen, V. L., White, D., Bramham-Law, C. W. F., Smith, V. C., 2014. Cryptotephra as a dating and correlation tool in archaeology. J Archaeol Sci 42, 42–50. https://doi.org/10.1016/j.jas.2013.10.033.

Langdon, P.G., Barber, K.E., 2001. New Holocene tephras and a proxy climate record from a blanket mire in northern Skye, Scotland. J Quat Sci 16, 753–759. https://doi.org/10.1002/jqs.655.

Langdon, P.G., Barber, K.E., 2004. Snapshots in time: precise correlations of peat-based proxy climate records in Scotland using mid-Holocene tephras. Holocene 14, 21–33. https://doi.org/10.1191%2F0959683604hl686rp.

Lawson, I.T., Swindles, G.T., Plunkett, G., Greenberg, D., 2012. The spatial distribution of Holocene cryptotephras in north-west Europe since 7 ka: implications for understanding ash fall events from Icelandic eruptions. Quat Sci Rev 41, 57–66. https://doi.org/10.1016/j.quascirev.2012.02.018.

Le Bas, M.J., Le Maitre, R.W., Streckeisen, A., Zanettin, B., 1986. A chemical classification of volcanic rocks based on the total alkali-silica diagram. J Petrol 27, 745–750. http://dx.doi.org/10.1093/petrology/27.3.745.

Lerbekmo, J.F., 2008. The White River Ash: largest Holocene Plinian tephra. Can J Earth Sci 45, 693–700. https://doi.org/10.1139/E08-023.

Lowe, D.J., 2011. Tephrochronology and its application: A review. Quat Geochronol 6, 107–153. https://doi.org/10.1016/j.quageo.2010.08.003.

Mangerud, J., Lie, S.E., Furnes, H., Kristiansen, I.L., Lømo, L., 1984. A Younger Dryas Ash Bed in western Norway, and its possible correlations with tephra in cores from the Norwegian Sea and the North Atlantic. Quat Res 21, 85–104. https://doi.org/10.1016/0033-5894(84)90092-9.

Nielsen, C. H., Sigurdsson, H., 1981. Quantitative methods for electron microprobe analysis of sodium in natural and synthetic glasses. Am Mineral 66, 547–552.

Patterson, R.T., Crann, C.A., Cutts, J.A., Courtney Mustaphi, C.J., Nasser, N.A., Macumber, A.L., Galloway, J.M., Swindles, G.T., Falck, H., 2017. New occurrences of the White River Ash (east lobe) in Subarctic Canada and utility for estimating freshwater reservoir effect in lake sediment archives. Palaeogeogr Palaeoclimatol Palaeoecol 477, 1–9. https://doi.org/10.1016/J.PALAEO.2017.03.031.

Pilcher, J., Bradley, R. S., Francus, P., Anderson, L., 2005. A Holocene tephra record from the Lofoten Islands, arctic Norway. Boreas 34, 136–156. https://doi.org/10.1111/j.1502-3885.2005.tb01011.x.

Pilcher, J.R., Hall, V.A., 1996. Tephrochronological studies in northern England. Holocene 6, 100–105. https://doi.org/10.1177/095968369600600112.

Pilcher, J.R., Hall, V.A., McCormac, F.G., 1995. Dates of Holocene Icelandic volcanic eruptions from tephra layers in Irish peats. Holocene 5, 103–110. https://doi.org/10.1177/095968369500500111.

Plunkett, G.M., Pilcher, J.R., McCormac, F.G., Hall, V.A., 2004. New dates for first millennium BC tephra isochrones in Ireland. Holocene 14, 780–786.

https://doi.org/10.1191%2F0959683604hl757rr.

Plunkett, G., Pilcher, J.R., 2018. Defining the potential source region of volcanic ash in northwest Europe during the Mid- to Late Holocene. Earth-Sci Rev 179, 20–37. https://doi.org/10.1016/j.earscirev.2018.02.006.

Rach, O., Brauer, A., Wilkes, H., Sachse, D., 2014. Delayed hydrological response to Greenland cooling at the onset of the Younger Dryas in western Europe. Nature Geoscience 7, 109. https://doi.org/10.1038/ngeo2053.

Reilly, E., Mitchell, F.J., 2015. Establishing chronologies for woodland small hollow and mor humus deposits using tephrochronology and radiocarbon dating. Holocene 25, 241–252. https://doi.org/10.1177/0959683614557571.

Rose, N. L., Golding, P. N. E., Battarbee, R. W. 1996. Selective concentration and enumeration of tephra shards from lake sediment cores. Holocene 6, 243–246. https://doi.org/10.1177/095968369600600210.

Sigl, M., Winstrup, M., McConnell, J. R., Welten, K. C., Plunkett, G., Ludlow, F., Büntgen, U., Caffee, M., Chellman, N., Dahl-Jensen, D., Fischer, H., Kipfstuhl, S., Kostick, C., Maselli, O. J., Mekhaldi, F., Mulvaney, R., Muscheler, R., Pasteris, D. R., Pilcher, J. R., Salzer, M., Schüpbach, S., Steffensen, J. P., Vinther, B. M., Fischer, H., 2015. Timing and climate forcing of volcanic eruptions for the past 2,500 years. Nature 523, 543. https://doi.org/10.1038/nature14565.

Swindles, G. T., Savov, I. P., Connor, C. B., Carrivick, J., Watson, E., Lawson, I. T., 2013. Volcanic ash clouds affecting Northern Europe: the long view. Geology Today 29, 214–217. https://doi.org/10.1111/gto.12026.

Szumański, A., 2000. Objaśnienia do Szczegółowej Mapy Geologicznej Polski, Arkusz Giżycko (104) . Państwowy Instytut Geologiczny, Warszawa.

Toohey, M., Sigl, M., 2017. Volcanic stratospheric sulfur injections and aerosol optical depth from 500 BCE to 1900 CE. Earth Syst Sci Data 9, 809–831. https://doi.org/10.1594/WDCC/eVolv2k_v2.

Turney, C. S. M., 1998. Extraction of rhyolitic ash from minerogenic lake sediments. J Paleolimnol 19, 199–206. https://doi.org/10.1023/A:1007926322026.

Tylmann, W., Bonk, A., Goslar, T., Wulf, S., Grosjean, M., 2016. Calibrating ^{210}Pb dating results with varve chronology and independent chronostratigraphic markers: problems and implications. Quat Geochronol 32, 1–10. https://doi.org/10.1016/j.quageo.2015.11.004.

van den Bogaard, C., Schmincke, H.-U., 2002. Linking the North Atlantic to central Europe: a high-resolution Holocene tephrochronological record from northern Germany. J Quat Sci 17, 3–20. https://doi.org/10.1002/jqs.636.

Vorren, K. D., Blaauw, M., Wastegård, S., Plicht, J. V. D., Jensen, C., 2007. High-resolution stratigraphy of the northernmost concentric raised bog in Europe: Sellevollmyra, Andøya, northern Norway.

Boreas 36, 253–277. https://doi.org/10.1111/j.1502-3885.2007.tb01249.x.

Wacnik, A., Tylmann, W., Bonk, A., Goslar, T., Enters, D., Meyer-Jacob, C., Grosjean, M., 2016. Determining the responses of vegetation to natural processes and human impacts in north-eastern Poland during the last millennium: combined pollen, geochemical and historical data. Veg Hist Archaeobot 25, 479–498. https://doi.org/10.1007/s00334-016-0565-z.

Wastegård, S., 2005. Late Quaternary tephrochronology of Sweden: A review. Quat Int 30, 49–62. https://doi.org/10.1016/j.quaint.2004.04.030.

Wastegård, S., Johansson, H., Pacheco, P. 2020. New major element analyses of proximal tephras from the Azores and suggested correlations with cryptotephras in Northwestern Europe. J Quat Sci 35, 114-121. DOI: 10.1002/jqs.3155.

Watson, E.J., Swindles, G.T., Lawson, I.T., Savov, I.P., 2016. Do peatlands or lakes provide the most comprehensive distal tephra records? Quat Sci Rev 139, 110–128. https://doi.org/10.1016/j.quascirev.2016.03.011.

Watson, E.J., Kołaczek, P., Słowiński, M., Swindles, G.T., Marcisz, K., Gałka, M., Lamentowicz, M., 2017a. First discovery of Holocene Alaskan and Icelandic tephra in Polish peatlands. J Quat Sci 32, 457–462. https://doi.org/10.1002/jqs.2945.

Watson, E.J., Swindles, G.T., Savov, I.P., Lawson, I.T., Connor, C.B., Wilson, J.A., 2017b. Estimating the frequency of volcanic ash clouds over northern Europe. Earth Planet Sci Lett 460, 41–49. https://doi.org/10.1016/j.epsl.2016.11.054.

Wulf, S., Dräger, N., Ott, F., Serb, J., Appelt, O., Gudmundsdóttir, E., van den Bogaard, C., Słowiński, M., Błaszkiewicz, M., Brauer, A., 2016. Holocene tephrostratigraphy of varved sediment records from Lakes Tiefer See (NE Germany) and Czechowskie (N Poland). Quat Sci Rev 132, 1–14. https://doi.org/10.1016/j.quascirev.2015.11.007.

Wulf, S., Ott, F., Słowiński, M., Noryśkiewicz, A.M., Dräger, N., Martin-Puertas, C., Czymzik, M., Neugebauer, I., Dulski, P., Bourne, A.J., Błaszkiewicz, M., Brauer, A., 2013. Tracing the Laacher See Tephra in the varved sediment record of the Trzechowskie palaeolake in central Northern Poland. Quat Sci Rev 76, 129–139. https://doi.org/10.1016/j.quascirev.2013.07.010.

Żarczyński, M., Tylmann, W., Goslar, T., 2018. Multiple varve chronologies for the last 2000 years from the sediments of Lake Żabińskie (northeastern Poland) – Comparison of strategies for varve counting and uncertainty estimations. Quat Geochronol 47, 107–119. https://doi.org/10.1016/J.QUAGEO.2018.06.001.

Żarczyński, M., Wacnik, A., Tylmann, W., 2019. Tracing lake mixing and oxygenation regime using the Fe/Mn ratio in varved sediments: 2000 year-long record of human-induced changes from Lake Żabińskie (NE Poland). Sci Total Environ 657, 585–596. https://doi.org/10.1016/j.scitotenv.2018.12.078.